AMSE JOURNALS-2016-Series: Modelling C; Vol. 77; N°1; pp 65-85
Submitted July 2016; Revised Oct. 15, 2016, Accepted Dec. 10, 2016

Seismic Liquefaction Study of Sandy Soil and its Application Research

ZHANG Weiping [1], SUN Jiawen[2], SUN Zhaochen[3*]

(1, 3. State Key Laboratory of Coastal and Offshore Engineering, Dalian University of Technology, Dalian 116024, China (e-mail: 368252227@qq.com)
2. The National Marine Environmental Monitoring Center, Dalian 116023, China

Abstract

As one of the most common particulate materials, sandy soil is widely distributed in natural geological environment. Compared with typical clayey soil, which has different mechanical properties and more tends to liquefy. In order to investigate the distinct mechanical properties, as well as the liquefaction resistance of sandy soil, with the introducing of subloading surface concept, the subloading surface Cam-clay model was introduced based on the classical Cam-clay model. Through precisely simulates the distinct evolution of *OCR*, which provides a practical method to simulate different type soils in a unified theoretic framework. And based on the parametric studies of mechanical properties and seismic liquefaction of clayey and sandy soils, two seismic simulation examples are carried out, owing to the faster rising of excess pore water pressure in sandy soil foundation, especially under the coupled interaction between structure and foundation soil, which leads to more significant strength degradation of foundation soil, results in larger seismic response and more severe force condition of structure under earthquake incident.

Key words

sandy soil; earthquake; seismic liquefaction; *OCR*; subloading surface Cam-clay model

1. Introduction

Among the major concerns in civil engineering, the seismic response of structure under earthquake incident was recognized as one of the most important issues in the design of civil

engineering structures (Rovithis, Pitilakis et al. 2009, Tang, Ling et al. 2010). Especially in coastal and offshore area or other saturated geological environment with sandy soil, owing to the strength degradation of foundation along with the rapid rising of excess pore water pressure under earthquake incident, which could leads to severe damage and even sudden collapse to civil engineering structures, such as tall buildings, bridges, wharfs and ocean platforms (Lu and Jeng 2010, Pan, Chen et al. 2011, Memarpour, Kimiaei et al. 2012). In the seismically induced liquefaction cases that occurred in the past few decades, it was found responsible for the damage and destruction of civil engineering facilities that happened in Japan's Niigata earthquake (1964), Loma Prieta earthquake (1989), Kobe earthquake (1995). And recently, the damages occurred in 2010 Canterbury earthquake and more extensively again that followed in 2011 were founded related with seismic induced liquefaction (Bardet and Kapuskar 1993, Fukusumi, Ozaki et al. 2002, Maurer, Green et al. 2015). Meanwhile, many similar observations derived from laboratory experiments also had been reported (Zhou, Chen et al. 2009, Gao, Ling et al. 2011). These reported failures and laboratory experimental observations induced by seismic liquefaction suggest that a more comprehensive understanding of the mechanism of seismic liquefaction, as well as the distinct liquefaction resistance of different soils is required to ensure the foundation able to resist the possible liquefaction and has enough bearing capacity to support the upper structure.

For seismic liquefaction of saturated soil as a result of the coupled interaction between soil skeleton and fluid pore water, when the excess pore water pressures rise to an extent exceed the contact stress between the grains of soil that keep them in contact with each other, which may results in a complete loss of soil strength (Matasovic and Vucetic 1995, Wang and Lou 2000), and which can be happed in sudden and catastrophic. And particularly, which is more likely to occur in sandy soil foundation (Sassa and Sekiguchi 2001, Xia, Ye et al. 2010). And in practical civil engineering, according to the different physical and mechanical properties, most soils were categorized into clayey or sandy soil, and simulated with different models, which brings lots of inconvenience to civil engineering practices, therefore, a concise and generalized constitutive model is required.

Among the various elastoplastic constitutive models of soil, the classic Cam-clay model was undoubtedly well known as the first practical constitutive model which could be able to provide an accurate description of clayey soil under normally consolidated state (Roscoe, Schofield et al. 1958, Zhang 2007). However, when confront with overconsolidated soil, or typical sandy soil material, which no longer be able to provide a satisfactory description (Zhang 2007, Vithana, Nakamura et al. 2012). Based on the Cam-clay model, subloading surface Cam-clay model was proposed with the

introducing of subloading surface concept (Asaoka, Nakano et al. 2006, Yamakawa, Hashiguchi et al. 2010). In this constitutive model, through precisely simulate the distinct evolution process of overconsolidation ratio (*OCR*) in different type soils, both clayey and sandy soils all can be modeled by this unified theoretical framework (Nakai and Hinokio 2004, Choo and Burns 2014).

Considering the great influence of seismic liquefaction in the design of important civil engineering infrastructures, at the same time, considering the distinct liquefaction resistance of different type soils, in order to study the mechanism of seismic liquefaction and the corresponding influence on the dynamic response of structure, based on the comparative studies of clay and sandy soils, then with the development of subloading surface Cam-clay model, a unified 3D nonlinear dynamic FEM program based on ADINA81 was established, under this FEM framework, two seismic simulation examples of a free field and a pier structure are conducted in this paper.

2. Subloading surface Cam-clay model

In the development history of soil constitutive model, the well-known Cam-clay model was one of the most widely used elastoplastic model applied in civil engineering (Zhang 2007). As developed from the laboratory experiment on remold clay, which could precisely simulate the yield process of normally consolidated clayey soil, while confronted with overconsolidated soil or typical sandy soil, which cannot be able to provide a satisfactory description anymore.

As a reflection of stress history, the overconsolidation factor plays a very important role in the mechanical properties of soil, based on Cam-clay model, with the proposed concept of subloading yield surface, the subloading surface Cam-clay model provides a practical method to simulate the mechanical properties of soil in a wider application scope by taking overconsolidation factor into consideration. In the determination of the governing equation of subloading yield surface, assuming the subloading yield surface and normally consolidated surface are geometric similar (Fig.1), thenthe governing equations for both normally consolidated yield surface and the subloading yield surface can be written as (Zhang 2007):

$$f = C_p \ln \frac{p}{p_0} + D^* \eta = 0 \tag{1}$$

$$f_s = C_P \ln \frac{p}{p_{N1}} + D^* \frac{q}{p} = 0 \tag{2}$$

Where $C_P = \frac{\lambda - k}{1 + e_0}$, $D^* = \frac{C_P}{M^*}$, M^* is the critical shear stress ratio, p and q are the mean effective stress and shear stress，parameter $\eta = q / p$ is shear stress ratio, e_0 is the porosity ratio of soil

under reference pressure p_0(98kPa), $\lambda = 0.434C_c$, $\kappa = 0.434C_s$, in which C_c and C_s are the volumetric compressibility and expansion coefficient, respectively.

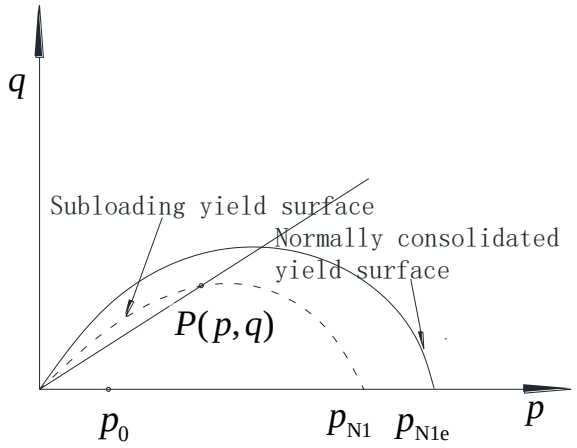

Fig.1 Yield surfaces of soil under different overconsolidated state

According to the relationship between stresses，the governing equation of subloading yield surface through stress point $P(p,q)$ could be written as：

$$f_s = C_P\left[\ln\frac{p}{p_0} - (\ln\frac{p_{N1e}}{p_0} - \ln\frac{p_{N1e}}{p_{N1}})\right] + D^*\frac{q}{p} = 0 \tag{3}$$

In the loading process from p_0 to p_{N1e} (Fig.1b), the plastic volume strain under isotropic compression could be derived through equation $\varepsilon_V^p = C_P \ln\frac{p_{N1e}}{p_0}$. Then through the relationship of stress and over consolidation parameter of $R(1/OCR,\ OCR = \frac{p_{N1e}}{p_{N1}})$, the governing equation of sub loading yield surface could be rewritten as:

$$f_s = \ln\frac{p}{p_0^*} + \frac{1}{M^*}\frac{q^*}{p^*} - \frac{1}{C_\mathrm{p}}\varepsilon_\mathrm{V}^\mathrm{p} - \ln R = 0 \tag{4}$$

Convert the governing equation from (p,q) stress space into general stress space (σ_m, J_2), then a more practical equation of sub loading yield surface in general stress space could be derived as：

$$f_s = \ln\frac{\sigma_m}{\sigma_{m0}^*} + \frac{\sqrt{3}}{M^*}\frac{\sqrt{J_2}}{\sigma_m} - \frac{1}{C_\mathrm{p}}\varepsilon_V^p - \ln R = 0 \tag{5}$$

Where $\sigma_m = \frac{\sigma_{ii}}{3}$, $J_2 = \frac{1}{2}s_{ij}s_{ij}$, $s_{ij} = \sigma_{ij} - \sigma_m$.

With taking the influence of over consolidation factor into consideration, the sub loading surface

Cam-clay model provides a practical method to describe the mechanical properties of soil under overconsolidated state. While for the evolution of parameter *R*, as it closely related with plastic strain, by Nakai *et al*'s advices (Nakai and Hinokio 2004, Asaoka, Nakano et al. 2006), assumes that $\mathrm{d}R = U\mathrm{d}\varepsilon_d^p$, and in which $U = -m_R \ln R \cdot \dfrac{M^*}{C_\mathrm{p}}$, where m_R is the material parameter which controlled the evolution rate of *OCR*. The evolution equation defined the derivative of *R* as a positive scalar function in terms of plastic stretching, as long as soil under plastic loading, which will always towards the direction of normally consolidated state. From the definition functions, it's clear to see that the larger value of parameter m_R means the quicker evolution rate of over consolidation in soil. And in typical clayey soil, there is a more rapid loss of over consolidation. Conversely, in sandy soil, the loss of over consolidation is assumed to occur slowly (Asaoka, Nakano et al. 2006).

Based on the governing equation of sub loading surface Cam-clay model, along with the evolution of *OCR*, then we could obtain the elastoplastic constitutive equation though coordination equation combined with Hooke's law:

$$\begin{aligned} \mathrm{d}\sigma_{ij} &= E_{ijkl}\mathrm{d}\varepsilon_{kl}^e = E_{ijkl}(\mathrm{d}\varepsilon_{kl} - \mathrm{d}\varepsilon_{kl}^p) \\ &= E_{ijkl}\mathrm{d}\varepsilon_{kl} - E_{ijkl}\Lambda\frac{\partial f}{\partial \sigma_{kl}} \end{aligned} \tag{6}$$

Where $\Lambda = \dfrac{\dfrac{\partial f}{\partial \sigma_{ij}} E_{ijkl}\mathrm{d}\varepsilon_{kl}}{h^p + \dfrac{\partial f}{\partial \sigma_{ij}} E_{ijkl} \dfrac{\partial f}{\partial \sigma_{kl}}}$, $h^p = \dfrac{1}{C_\mathrm{p}}\left\{\dfrac{\partial f}{\partial \sigma_{mm}} - \dfrac{m_R \ln R}{R}\dfrac{1}{\sigma_m}\right\}$, E_{ijkl} is the stiffness tensor, ε_{kl}, ε_{kl}^e and ε_{kl}^p are the total strain tensor, elastic strain tensor and plastic strain tensor, respectively.

Through the established constitutive equation, the corresponding elastoplastic loading criteria could subsequently be obtained as below:

$$\begin{aligned} &\text{Loading:}\ \left|\mathrm{d}\varepsilon_{ij}^p\right| > 0 \quad \begin{cases} \Lambda > 0,\ \mathrm{d}f_\sigma = \dfrac{\partial f}{\partial \sigma_{ij}}\mathrm{d}\sigma_{ij} > 0 & \text{Hardening} \\ \Lambda > 0,\ \mathrm{d}f_\sigma = \dfrac{\partial f}{\partial \sigma_{ij}}\mathrm{d}\sigma_{ij} < 0 & \text{Softening} \end{cases} \\ &\text{Unloading:}\ \left|\mathrm{d}\varepsilon_{ij}^p\right| = 0,\ \ \Lambda \le 0 \end{aligned} \tag{7}$$

3. Model verification and parametric analysis

With taking the influence of over consolidation into consideration, sub loading surface Cam-clay model provides a unified framework for extensive study of different type soils in wider application scope. In this part, the validity and reliability of sub loading surface Cam-clay model is verified firstly, and then through monotonic and cyclic loading tests, comparative studies are carried out on

both clayey and sandy soils under the unified theoretic framework.

3.1 Model verification and parametric study of m_R

Firstly, in order to verify the validity and reliability of sub loading surface Cam-clay model in the simulation of clayey and sandy soils, triaxial compression tests with constant mean principal stress (p=196kPa) are carried out on Fujinomori clay and Toyoura sand (Table.1) (Asaoka, Nakano et al. 2006).

Table 1 Material parameters of soil samples

Item	Fujinomori clay	Toyoura sand
Compression index (λ)	0.09	0.07
Swelling index (κ)	0.02	0.005
Critical shear stress ratio (M^*)	1.36	1.5
Parameter of *OCR* (m_R)	2.1	0.2
Void ratio at 98kPa (e_0)	0.83	1.1
Poisson's ratio (ν)	0.2	0.2

In the loading test of Fujinomori clay, four soil samples with one normally consolidated soil sample (*OCR*=1) and three overconsolidated soil samples (*OCR*=2, 4, 8) are used. The comparison of laboratory observed results and numerical predictions by sub loading surface Cam-clay model are shown in Fig.2. From the loading responses it can be seen that the laboratory test observations and numerical predicted results are in good agreement, the strength softening and volume dilatancy phenomenon of overconsolidated soil are well simulated with good precision. As it can be seen from the response of stress-strain relationship curves (Fig.2a), compared with the normally consolidated soil sample, the overconsolidated soil samples all experiences a notable strength hardening process with higher yield strength (q/p=1.36, 1.53, 1.72, 1.92), and once the stress-strain curves reaches the apex point, along with the decay of *OCR* in the plastic loading process, the yield strength decreases accordingly, and the ultimate yield strength all approaches to the same stress level that performed in normally consolidated soil sample.

Fig.2b shows the corresponding volume compression during the loading process. As it can be seen from the comparison curves, the normally consolidated soil sample shows the highest compressibility (Δe = -3.4%), while for the overconsolidated soil samples, which all experienced an obvious reversion in the compression process, the void ratio was compressed at the first loading stage, while with the loading keeps continuing, especially with larger initial *OCR*, which began to increase and displays obvious volume dilatancy in the end (Δe = 1.19%, 2.41%, 3.21%). Through the comparative loading tests, it could be derived that the predicted strength degradation and dilatancy phenomenon along with the stress-strain response well proved the reliability and accuracy

of sub loading surface Cam-clay model, with taking over conslidation factor into consideration, which provides a practical method to simulate the loading response of soil under overconsolidated state.

Fig.3 shows the test results of Toyoura sand, as it can be seen from the loading responses, both stress-strain response and dilatancy phenomenon of loose sand and dense sandy soil samples are well simulated by sub loading surface Cam-clay model, and the dense sand shows much higher yield strength (*q/p*=1.74, 1.45) and demonstrates larger dilatancy in the yielding process. Through verification and parametric study on both clayey and sandy soil samples, it can be concluded that through choses proper material parameter of *OCR* (m_R), the sub loadng surface Cam-clay model provides a practical and precise model to simulate the distinct mechanical properties of sandy soil in a unified theoretic framework.

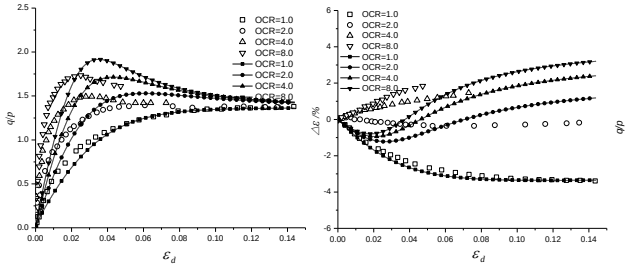

a $\varepsilon_d - q/p$ b $\varepsilon_d - \Delta e$

Fig.2 Triaxial test of Fujinomori clay

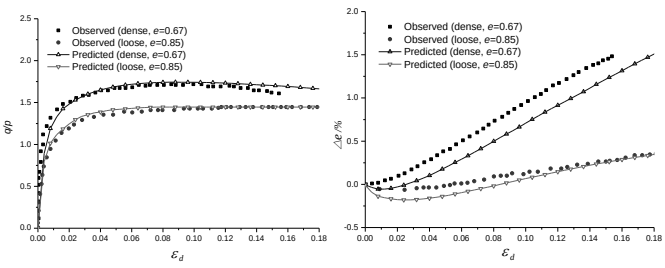

a $\varepsilon_d - q/p$ b $\varepsilon_d - \Delta e$

Fig.3 Triaxial test of Toyoura sand

Considering the loading responses of both clayey and sandy soils are well simulated by sub loading surface Cam-clay model through taking the effect of over consolidation factor into consideration, in this part, through choses appropriate parameter m_R (Table 2), both drained and undrained triaxial loading tests are conducted on three different type soil samples (from typical clayey soil to sandy soil) under the unified theoretic framework of sub loading surface Cam-clay model. And the mechanical parameters all share the same value as that of Fujinomori clay except m_R, and the initial *OCR* are set to 4.0 (*R*=0.25) to simulate the initial overconsolidated state.

Table 2 State variable parameter of soil samples

Soil samples		m_R
Clay	sample 1	2.0
↓	sample 2	0.5
Sand	sample 3	0.1

The drained loading test results are shown in Fig.4. In the loading response of *q/p*-ε_d (Fig.4a), it can be seen that all the soil samples experience a notable strength softening process, and which displays more obviously and reaches higher shear stress ratio in the clayey soil sample (Sample 1,

ε_d =0.020, *q/p*=1.76) than that demonstrated in the sandy soil sample (Sample 3, ε_d =0.096, *q/p*=1.52). Apart from the stress-strain response, the development of void ratio and the corresponding evolution of *OCR* are also derived along with the loading process. From the compression curves in Fig.4b, it can be seen that at the first loading stage, all soil samples experience an obvious volume shrinkage process under shear stress loading ($\Delta e = (\lambda - k) / M^* \cdot \eta$), while with the loading keeps proceeding, the volume expansion due to the decay of *OCR* gradually dominates the compressibility characteristics of soil ($\Delta e = C_P(1+e_0)\ln OCR$), and then the compression response of overconsolidated soil is a combination of the volume shrinkage part due to shear loading and the expansion part due to the decay of *OCR*. At the same time, owing to the distinct evolution rate of *OCR* in different soil samples (Fig.4c), the volume compression curves follow distinct development paths. However, all soil samples reach the same void ratio and normally consolidated state after yield.

The undrained loading test results are shown in Fig.5. As the buildup of excess pore water pressure is closely related with the compression of soil skeleton, then the buildup curves of excess pore water pressure also experiences a notable reversion in the yield process, and displays negative pressure in the end. And owing to distinct compressibility of clayey and sandy soils, the maximum excess pore water pressure reached 9.3kPa and 43.0kPa in the two soil samples. At the same time, owing to the influence of excess pore water pressure, which significantly accelerates the decay of *OCR* and displays smaller shear strength (Sample 1, ε_d =0.015, *q/p*=1.67; Sample 3, ε_d =0.035, *q/p*=1.44).

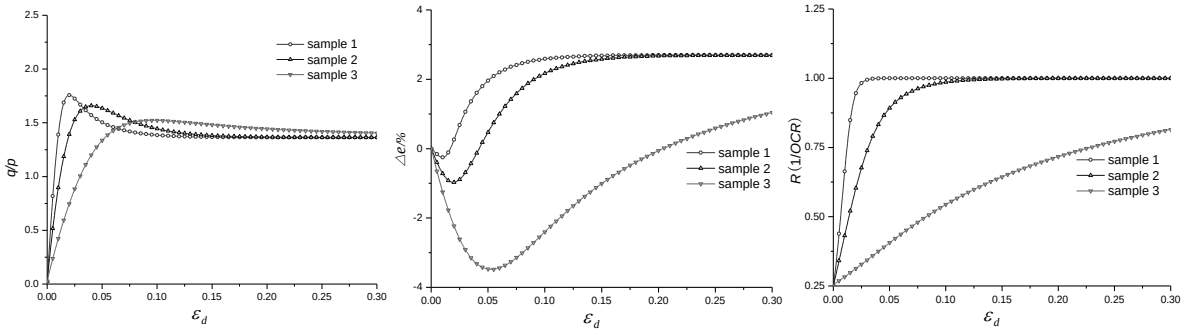

a $\varepsilon_d - q/p$ b $\varepsilon_d - \Delta e$ c $\varepsilon_d - R$

Fig.4 Drained triaxial test with constant mean principal stress

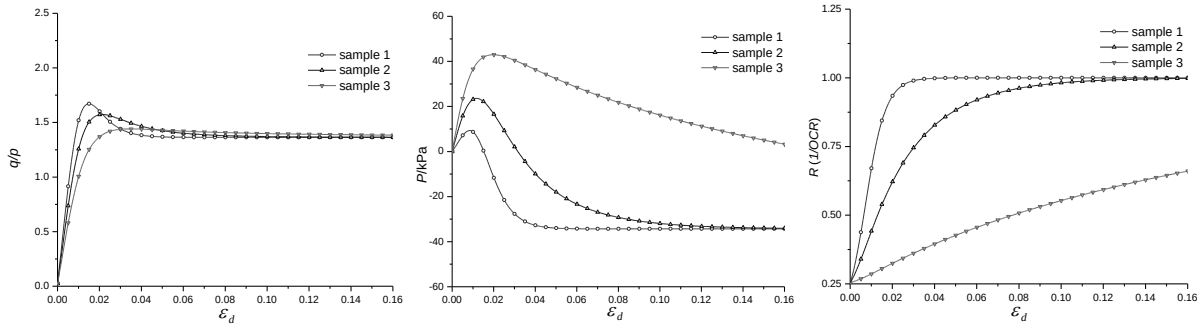

a $\varepsilon_d - q/p$ b $\varepsilon_d - P$ c $\varepsilon_d - R$

Fig.5 Undrained triaxial test with constant mean principal stress

3.2 Cyclic loading response and seismic liquefaction study of clayey and sandy soils

Considering the dangerous destructive power of seismic liquefaction, as well as the distinct liquefaction resistance of clayey and sandy soils, therefore, correct estimation of foundation's bearing capacity under earthquake incident is necessary for the seismic design of important soil structures in liquefiable geological environments. In this part, both drained and undrained cyclic loading tests are conducted on both typical clayey and sandy soil samples (Sample 1 and Sample 3, Table.2) with specific *OCR* value (*OCR*=1, 2, 4). In the loading tests, total 3000 steps with incremental strain step $\Delta\varepsilon_d = 0.002$ and loading stress amplitude (σ_1-σ_3) of 20kPa are carried out.

Firstly, the drained cyclic loading test is conducted and the test results of both clayey and sandy soils are presented in Fig.6 and Fig.7, respectively. From the stress-strain response curves in Fig.6a and Fig.7a, it can be seen that with the increases of *OCR*, the soil samples demonstrate much better mechanical performance and smaller compressibility under the cyclic loading test. At the same time, from the comparison between clayey and sandy soil samples, it also can be found that the sandy soil samples shown stronger nonlinearity characteristics and larger compressibility (Δe= 0.40, 0.32 and 0.23) than clayey soil (Δe= 0.24, 0.16 and 0.08), the typical sandy soils can be compressed to higher density under cyclic loading. Meanwhile, as the evolution of *OCR* is closely related with the development of soil density, Fig.6d and Fig.7d present the corresponding evolution of *OCR* in the cyclic loading test. Owing to the different evolution rate between clayey and sandy soils, in the sandy soil samples, the *OCR* reaches the stable state just after a few loading cycles, and the soil samples are compressed to more density state (*e*=0.44, 0.47, 0.51), while the evolution of *OCR* in clayey soil samples displays a more gradual evolution process and then the soil samples reaches a relative higher void ratio state after the loading test (*e*=0.60, 0.63, 0.66).

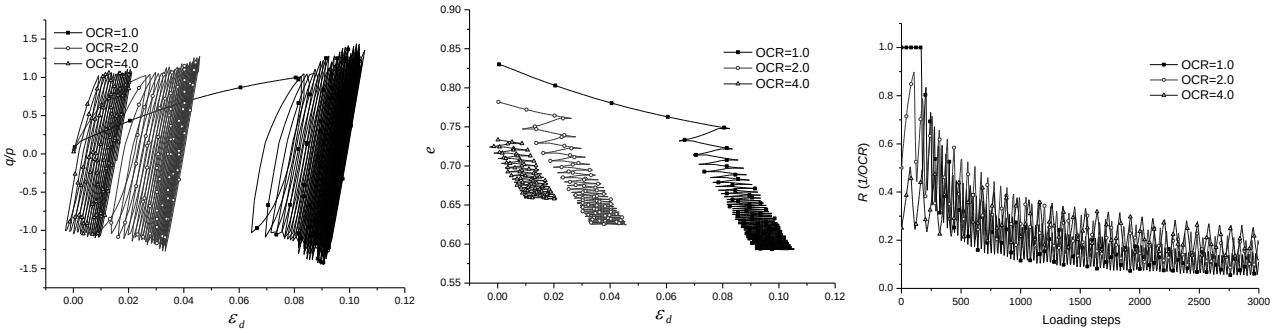

a $\varepsilon_d - q/p$ b $\varepsilon_d - e$ c R

Fig.6 Drained triaxial test of soil under cyclic loading (Clayey soil)

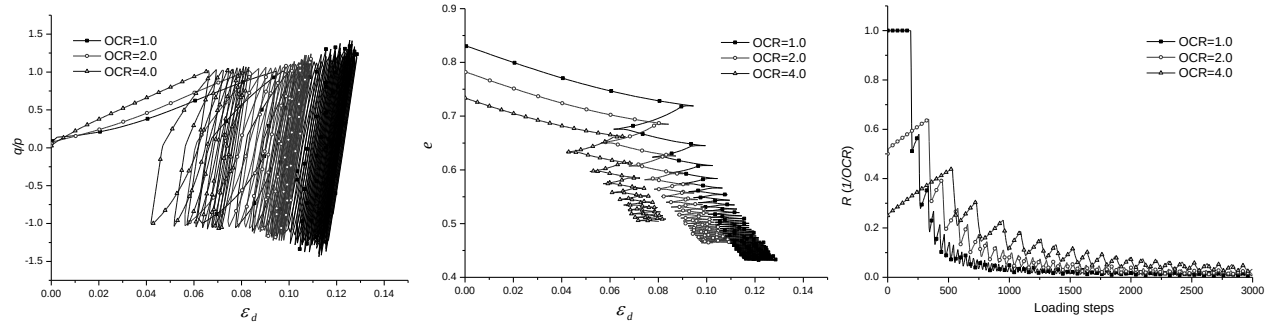

a $\varepsilon_d - q/p$ b $\varepsilon_d - e$ c R

Fig.7 Drained triaxial test of soil under cyclic loading (Sandy soil)

Secondly, since the distinct mechanical properties of clayey and sandy soils are found in drained loading tests, meanwhile, considering the buildup of excess pore water pressure as a result of dynamic coupled interaction between soil skeleton and fluid pore water, in order to further investigate the liquefaction mechanism and the distinct liquefaction resistance of different type soils, the undrained cyclic loading tests are conducted on both clayey and sandy soils and the comparative test results are presented in Fig.8 and Fig.9, respectively.

Unlike in the drained tests that all soil samples reached their respective stable state after several loading cycles, in the undrained loading test, along with the compression of soil skeleton, the loading pressure transferred to the fluid pore water, and then followed by the rising of excess pore water pressure (Fig.8b and Fig.9b), accordingly. With the decreases of soil effective stress, which accelerates the strength degradation of soil, until completely lost bearing capacity when reaches the critical state of liquefaction. Especially, owing to the larger compressibility, the normally consolidated soil samples reach the critical state of liquefaction more quickly. As well as the influence of *OCR*, the distinct mechanical properties between clayey and sandy soils are also reflected in the buildup of excess pore water pressure, the sandy soil samples almost liquefied just after few loading cycles (Fig.9b), while in the clayey soil samples, owing to the better mechanical

performance and lower compressibility, which enables the clayey soil samples maintained at a relative stable state after dozens of loading cycles (Fig.8a).

In order to further investigate the evolution of *OCR* under the influence of excess pore water pressure, the corresponding evolution curves of *OCR* are derived and presented in Fig.8c and Fig.9c, respectively. As it can be seen from the evolution curves, unlike in the drained test that *OCR* all reaches their final higher *OCR* state, in the undrained cyclic laoding test, at the first loading stage , with the quite small excess pore water pressure level, which has limited influence on soil's mechanical properties, as well as the evolution of *OCR*, while with the rapid rising of excess pore water pressure, which began to show significant influence on the evolution of *OCR*, particularly when approaches the critical liquefaction state, the develop of *OCR* reverses rapidly and degenerates into normally consolidated state, and which more likely to happen in sandy soil samples for the quicker rising of excess pore water pressure.

Through the comparative studies of the cyclic loading response of clayey and sandy soils, it can be concluded that through precisely simulates the evolution of *OCR*, the subloading surface Cam-clay model provides a practical unified theoretic framework to simulate the distinct mechanical properties and liquefaction resistance of different type soils. Compared with clayey soil, owing to the quicker rising of excess pore water pressure under cyclic loading, sandy soil responded with much more progressive degradation of soil strength until lost the whole strength when reaches the critical state of liquefaction.

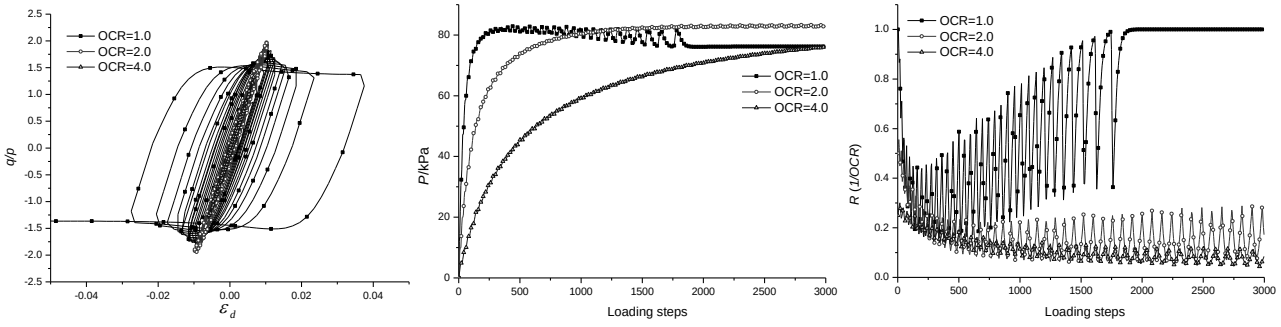

a $\varepsilon_d - q/p$ b P c R

Fig.8 Undrained test of soil under cyclic loading (Clayey soil)

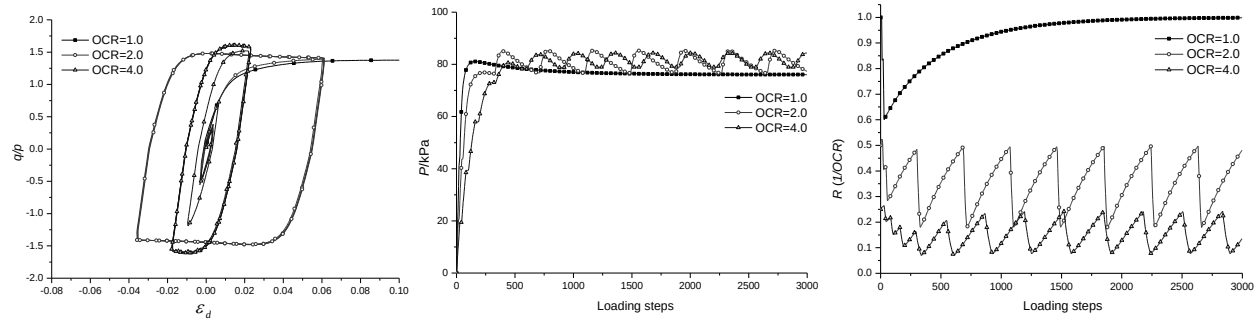

a $\varepsilon_d - q/p$ b P c R

Fig.9 Undrained test of soil under cyclic loading (Sandy soil)

4. Seismic simulation examples and discussions

Considering the great dangers of seismic liquefaction and the distinct liquefaction resistance of clayey sand sandy soils, then for the structures constructed in saturated foundation, particularly in sandy soil foundation, when subjected to earthquake incident, a flow failure may occur along with the rapid risingof excess pore water pressure in a short period of time. In this paper, with the development of subloading surface Cam-clay model, a 3D dynamic nonlinear FEM program based on open-source ADINA81 program is developed, which provides a unified framework for seismic study of structure in different type soil foundations. And then two seismic simulation examples of a free field and a pier structure are carried out on both clayey soil and sandy soil foundations (Sample 1 and Sample 3 in Table.2).

4.1 Example 1: Seismic analysis of free field

In this seismic simulation example, a homogeneous free field foundation with 30m depth is presented. In order to simulate the seismic wave propagation in half-space free field, viscoelastic artificial boundaries are added to the truncated cross sections. In the numerical model, a computational domain of 50m×20m×30m area with 960 8-node isoparametric elements is used (Fig.10). And in the seismic simulation, scaled Loma wave (San Francisco Bay Area of California, 1989, 0.11g, Fig.11) with peak acceleration value of 0.2g is used to simulate the incident earthquake wave.

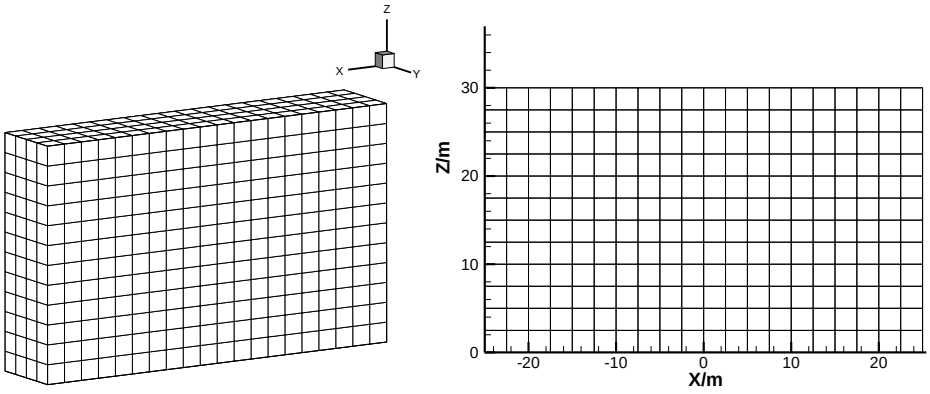

Fig.10 Mesh for finite element analysis

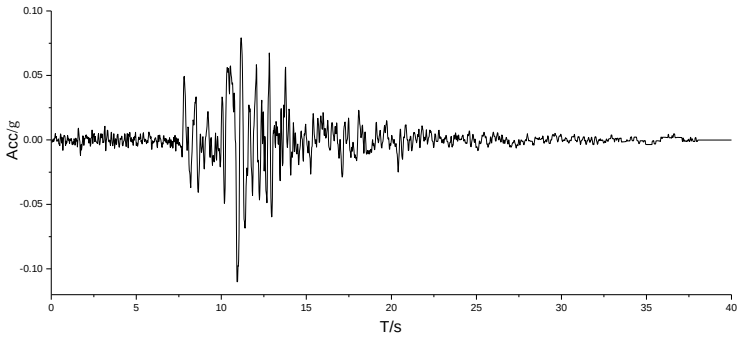

Fig.11 Time-history of input seismic acceleration

Fig.12 shows the seismic responses at ground surface derived from both clayey (Free field 1) and sandy soil foundations (Free field 2). As the two foundation soils used the same material parameters except m_R, in the early stage of earthquake incident, the seismic responses in the two fields are very close, while influenced by the distinct strength degradation along with the rising of excess pore water pressure, the sandy field foundation shows much stronger nonlinearity with the decreases of model's stiffness, and which significantly affects the dynamic characteristics of field foundation, the maximum acceleration reaches 4.09m/s^2 and 3.14m/s^2, and the corresponding maximum displacement reaches 0.11m and 0.07m, respectively in the two field foundations. As well as seismic response, the plastic deformations reached 0.01m and 0.03m after earthquake incident in the two field foundations, which almost tripled in the foundation case with sandy soil.

Fig.13 presents the distribution of excess pore water pressure ratio along field depth after earthquake incident, from the distribution curves it can be seen that the upper soil reaches higher excess pore water pressure, and with depth goes deeper, the distribution curves show exponential attenuation pattern from ground surface. Meanwhile, owing to the distinct liquefaction resistance between clay and sandy soils, which is directly reflected in the distribution curves of excess pore water pressure, especially in the upper zone near ground surface, the sandy soil free field almost liquefied near ground surface, while the difference of excess pore water pressure between the two fields decreases along with the increase of field depth.

Considering the significant difference of seismic response and liquefaction resistance between clayey and sandy soil foundations, in order to get a more comprehensive understanding of the buildup of excess pore water pressure and stress-strain response in different soil fields, the stress-strain relationship curves and the buildup curve of excess pore water pressure derived from 5m, 10m, 20m depth are presented in Fig.14, respectively. As it displayed in the figures, as the two field foundations used the same mechanical parameters, at the early stage of earthquake incident, the excess pore water pressure curves and stress-strain response are very close, while owing to the distinct liquefaction resistance of sandy soils, which directly reflected in the buildup of excess pore

water pressure, and significantly accelerates the strength degradation process of soil and influences the dynamic characteristics of field foundation under earthquake incident, accordingly.

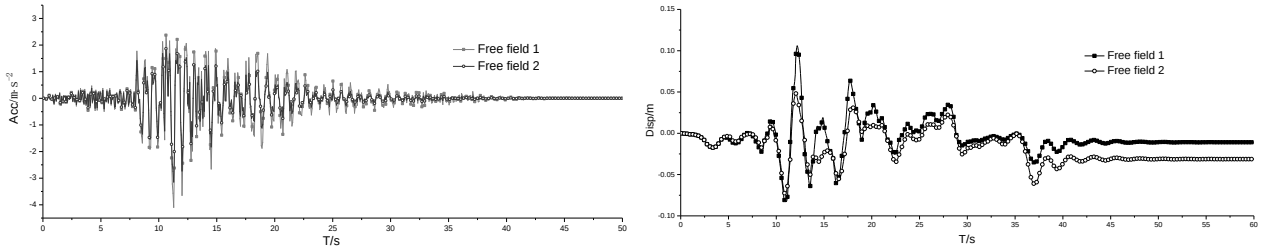

a Acceleration b Displacement

Fig.12 Dynamic response of ground surface

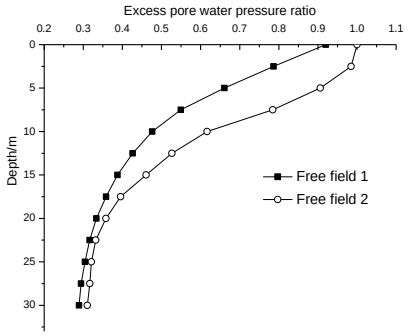

Fig.13 Distribution of excess pore water pressure

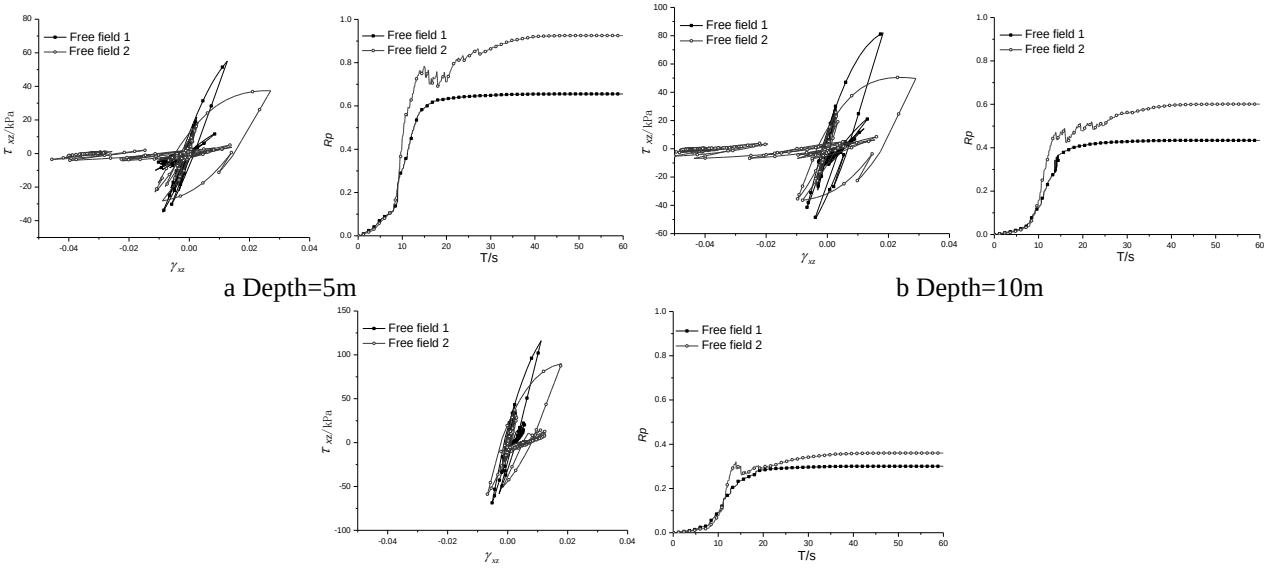

a Depth=5m b Depth=10m

c Depth=20m

Fig.14 Seismic response of foundation soil

4.2 Example 2: Seismic analysis of pier structure

In this numerical example of a simplified offshore pier structure, the supporting piles are driven to 20m deep below ground surface, and the layout of piles was set to 18m×12m arrangement, the piles were made of steel pipe with diameter of 2.8m and thickness of 32mm, the Yong's modulus is 210GPa, the simplified upper structure weights 2000KN. In the simulation of seismic motion in half-space soil foundation, a 100m×40m×30m calculation domain with viscoelastic artificial boundaries is used. And considering the symmetry of calculation model, just one-half domain of the numerical model is taken for FEM calculation, and then the numerical model was discretised into 3888 nonlinear 8-node isoparametric elements for soil foundation, and 584 elastic elements for simplified pier structure (Fig.15). In this seismic simulation, the scaled Loma wave with peak acceleration of 0.2g is also used as incident earthquake wave.

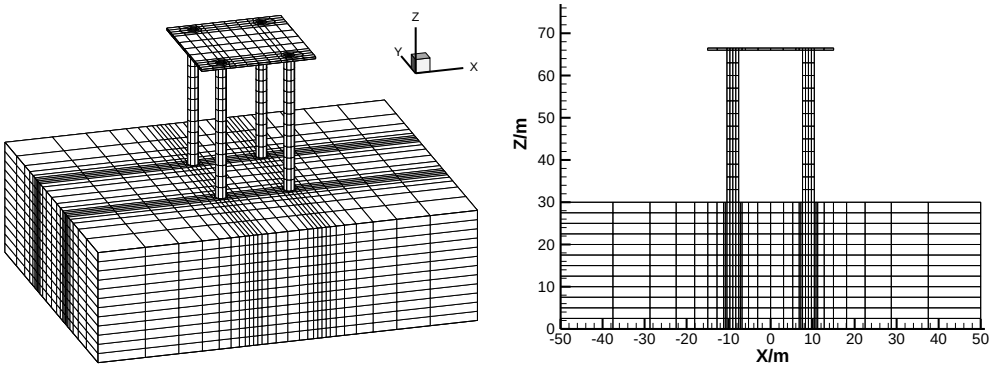

a FEM Model of a simplified pier b Cross-section of the pier model

Fig.15 Mesh for finite element analysis of the pier model

Firstly, the cloud contour maps of excess pore water pressure ratio derived from clayey soil foundation is illustrated in Fig.16, which provides an overall comprehension of the coupled pile-soil interaction in saturated foundation. As it displays in the contour maps, besides the attenuation of excess pore water pressure from ground surface, under the dynamic coupled interaction between piles and foundation soil, there shows obvious concentration of excess pore water pressure in the near field of structure.

Secondly, a more precise figure of excess pore water pressure ratio distribution curves derived from both clayey and sandy soil foundations is presented in Fig.17. Through the comparison of excess pore water pressure ratio derived from far field and near field, it can be seen that the coupled pile-soil interaction had significantly accelerates the buildup of excess pore water pressure, particularly in the sandy soil foundation, which had liquefied in the upper 2.5m near ground surface. With the depth goes deeper, as the motion of foundation soil and structure piles tend to synchronize, the corresponding influence of the coupled pile-soil interaction decreases accordingly, while it also should be noted that in the area of pile toe, the excess pore water pressure curve displays an obvious

vertex due to the stress concentration in the interface area of piles and foundation soil.

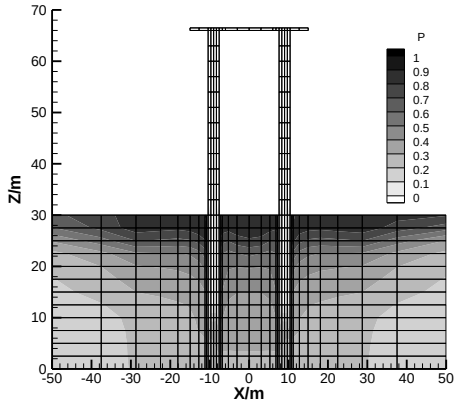

Fig.16 Excess pore water pressure ratio (t=60.0s)

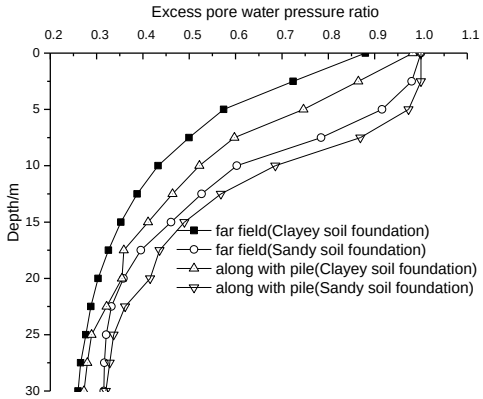

Fig.17 Distribution of excess pore water pressure ratio

Fig.18 shows the seismic response of structure's top node, in the comparative study, apart from the simulated results derived from clayey and sandy soil foundations, an ideal linear elastic soil foundation is also presented as a background reference (Young's modulus E is expressed in terms of the swelling index κ and Poisson's ratio ν as $E = \frac{3(1-2\nu)(1+e_0)p}{\kappa}$). In the seismic response curves, the maximum acceleration reaches 18.36m/s^2, 14.34m/s^2 and 11.23m/s^2, and the corresponding maximum displacement reaches 0.29m, 0.34m and 0.46m, respectively derived from elastic, clayey and sandy soil foundations. As well as seismic response, the horizontal plastic deformation reaches 0.04m and 0.08m in the clayey and sandy soil foundations. Compared with the ideal elastic foundation, particularly with sandy soil foundation, owing to the degradation of soil strength along with the rapid rising of excess pore water pressure, the distinct degradation of foundation's bearing capacity leads to more significant decreases of structure stiffness and subsequently affects the seismic response of the pier structure.

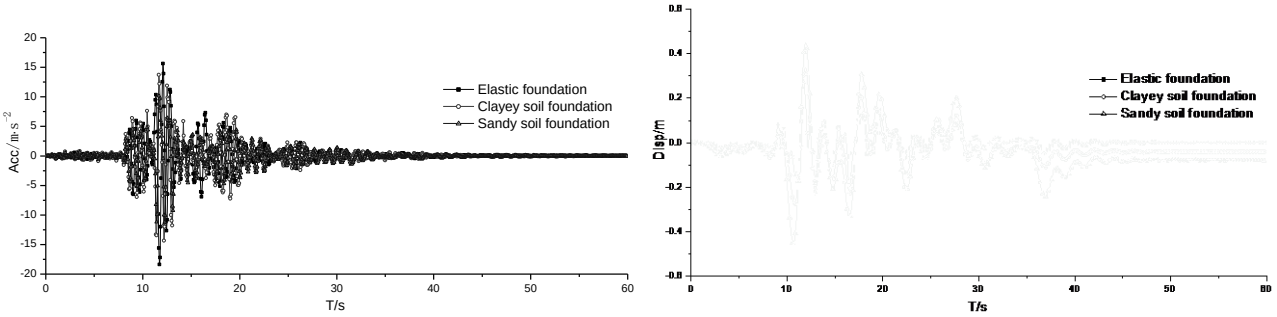

a Acceleration b Displacement

Fig.18 Dynamic response of the structure's top node

In view of the distinct seismic responses in clayey and sandy soil foundations, in order to further investigate the deflection and force condition of structure under earthquake incident, the maximum horizontal deflection and bending moment envelop of pile are derived in Fig.19. The pile reaches the maximum deflection of 0.29m, 0.34m and 0.46m at pile's top node in the three soil foundations, and the deflection curves show obvious inflection near ground surface (Fig.19a). Meanwhile, through stress integration in pile's cross section, similar comparative results of bending moment envelope are derived in Fig.19b. Aims to make the comparison be more comprehensible, the bending moment envelops are given in relative value, and the maximum bending moment derived from elastic foundation model (M_0) is used as background reference. From the figure it can be seen that the envelope curves all demonstrate two distinct peaks along pile length, and owing to the distinct degradation of foundation's bearing capacity, the pile reaches the maximum bending moment of 1.20 and 1.37 near ground surface in the clayey and sandy soil foundations, respectively. Therefore, in the geological environment with saturated sandy soil foundation, which should be paid more attention in the seismic design of structures to resist the possible seismic liquefaction and ensure the safety of structure.

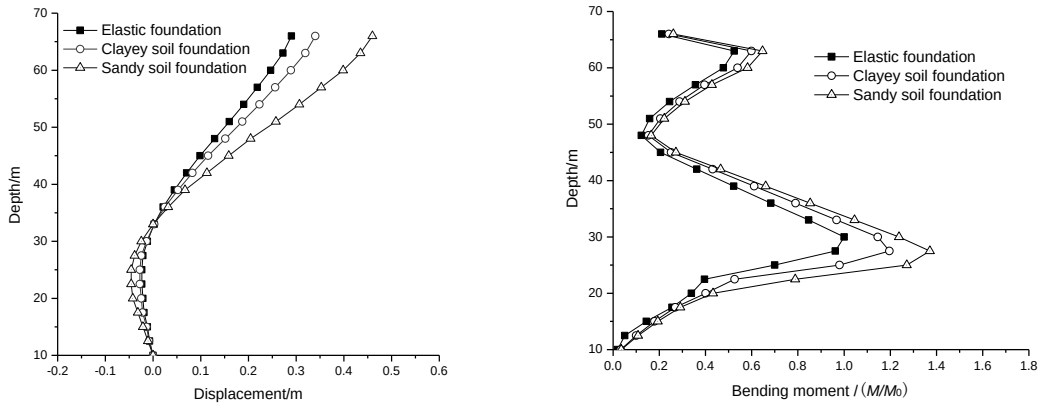

a Horizontal deflection b Moment envelope

Fig.19 Horizontal deflection and bending moment along with pile

5. Discussion

With considering the influence of over consolidation factor, as well as the distinct evolution ratio of *OCR* in different type soils, the predicted results by sub loading surface Cam-clay model are compared favourably with the experimental results of both clayey and sandy soils. Our results confirmed the feasibility of study the seismic liquefaction of clayey and sandy soils in a unified theoretic framework.

Considering the super loading surface Cam-clay model able to provide a unified model for both clayey and sandy soils by choosing proper evolution ratio of over consolidation, meanwhile, as the parameter of m_R is obtained through curve fitting on the loading response of soil, which cannot be directly derived through conventional laboratory experiment or other common parameters, therefore, a more practical method to determine the precise value of parameter m_R will be an important research issue in the future research.

Considering the seismic liquefaction of soil is a complex phenomenon of the coupled interaction between soil skeleton and fluid pore water, for the transient problem such as earthquake incidence, the undrained simplification of foundation soil without considering the pore flow in soil porosity is acceptable. While for the structures subjected to long period loads, such as wave, sea current flow as well as the long time dynamic working loads, the influence of pore flow, as well as the permeability of soil couldn't be neglected anymore. Under these circumstances, the problem is neither transient nor steady-state process, then the simulation of these problems will be very time consuming, how to simplify this problem will be the direction of future research.

6. Conclusions

With considering the effect of over consolidation as well as the distinct evolution ratio of *OCR* in different type soils, the sub loading surface Cam-clay model provides an available unified theoretic framework for the simulation of different soils in wider application scope. Based on the comprehensive studies of clayey and sandy soils, seismic simulation examples of a free field and a simplified pier structure are conducted, and the following conclusions are derived:

Through precisely simulates the influence and evolution of *OCR*, the sub loading surface Cam-clay model well revealed the mechanism of strength degradation and volume dilatancy phenomenon of overconsolidated soil, and with the increase of *OCR*, overconsolidated soil shows better mechanical performance and liquefaction resistance. Compared with clayey soil, sandy soil shows much stronger nonlinear characteristics, higher compressibility, and more tends to liquefy under cyclic loading.

In the seismic simulation examples of free field and pier structure, along with the faster rising of excess pore water pressure in sandy soil field foundation, especially under the coupled interaction between structure and foundation soil, the rapid rising of excess pore water pressure leads to more significant strength degradation of foundation soil and the decreases of structure's stiffness, which results in larger seismic response and more severe force condition of structure under earthquake incident.

Through the comprehensive investigation on clayey and sandy soils, as well as the seismic liquefaction study of soil foundation, it could be concluded that the sub loading surface Cam-clay model provides a practical method for extensive study of seismic liquefaction of different type soils in a unified framework. The conclusions derived from the comparative studies could provide some useful insights and references for the seismic design of civil engineering structures in liquefiable sandy soil foundation.

Acknowledgment

Project supported by the Foundation for Innovative Research Groups of the National Natural Science Foundation of China (Grant No. 51221961) and State Key Development Program of Basic Research of China (No. 2011CB013701).

References

1. Asaoka, A., M. Nakano and T. Noda (2006). "A Super/Subloading Yield Surface Approach to Compaction/Liquefaction of Sand and Secondary Consolidation of Clay[C]." Geomechanics II-Testing, Modeling and Simulation, Proceedings of the Second GI-JGS workshop, Osaka, ASCE Geotechnical Special Publication: 201-218.
2. Bardet, J. and M. Kapuskar (1993). "Liquefaction sand boils in San Francisco during 1989 Loma Prieta Earthquake." Journal of Geotechnical Engineering 119(3): 543-562.
3. Choo, H. and S. Burns (2014). "Effect of overconsolidation ratio on dynamic properties of binary mixtures of silica particles." Soil Dynamics and Earthquake Engineering 60: 44-50.
4. Fukusumi, T., H. Ozaki and M. Kobac (2002). "Influence of the ground profile on the reduction of earthquake motion at the filled man-made islands in the Kobe harbor during the 1995 Hyogoken Nambu earthquake." Journal of Soil Dynamics and Earthquake Engineering 22(893-899).

5. Gao, X., X. Ling, L. Tang and P. Xu (2011). "Soil-pile-bridge structure interaction in liquefying ground using shake table testing." Soil Dynamics and Earthquake Engineering 31(7): 1009-1017.
6. Lu, J. and D. Jeng (2010). "Dynamic response of an offshore pile to pseudo-Stoneley waves along the interface between a poroelastic seabed and sea water." Soil Dynamics and Earthquake Engineering 30(4): 184-201.
7. Matasovic, N. and M. Vucetic (1995). "Generalized cyclic-degradation-pore-pressure generation model for clays." Journal of Geotechnical Engineering 121(1): 33-42.
8. Maurer, B., R. Green, M. Cubrinovski and B. Bradley (2015). "Fines-content effects on liquefaction hazard evaluation for infrastructure in Christchurch, New Zealand." Soil Dynamics and Earthquake Engineering 76: 58-68.
9. Memarpour, M., M. Kimiaei, M. Shayanfar and M. Khanzadi (2012). "Cyclic lateral response of pile foundations in offshore platforms." Computers and Geotechnics 42: 180-192.
10. Nakai, T. and M. Hinokio (2004). "A simple elastoplastic model for normally and over consolidated soils with unified material parameters." Soils and Foundations 44(2): 53-70.
11. Pan, H., G. Chen and H. Liu (2011). "Behavior of large post-liquefaction deformation in saturated Nanjing fine sand." Earthquake Engineering and Engineering Vibration 10(2): 187-193.
12. Roscoe, K., A. Schofield and C. Wroth (1958). "On yielding of soils." Geotechnique 8(1): 22-53.
13. Rovithis, E., K. Pitilakis and G. Mylonakis (2009). "Seismic analysis of coupled soil-pile-structure systems leading to the definition of a pseudo-natural SSI frequency." Soil Dynamics and Earthquake Engineering 29(6): 1005-1015.
14. Sassa, S. and H. Sekiguchi (2001). "Analysis of wave-induced liquefaction of sand beds." Geotechnique 51(2): 115-126.
15. Tang, L., X. Ling and P. Xu (2010). "Shake table test of soil-pile groups-bridge structure interaction in liquefiable ground." Earthquake Engineering and Engineering Vibration 9(1): 39-50.
16. Vithana, S., S. Nakamura, S. Kimura and S. Gibo (2012). "Effects of overconsolidation ratios on the shear strength of remoulded slip surface soils in ring shear." Engineering Geology 131-132(29): 29-36.
17. Wang, S. and Z. Lou (2000). "Degradation of undrained shear strength of marine silty clay after undrained cyclic loading." Ocean Engineering 18(1): 38-43. (in Chinese)

18. Xia, Z., G. Ye and J. Wang (2010). "Numerical Analysis on the Influence of Thickness of Liquefiable Soil on Seismic Response of Underground Structure." Journal of Shanghai Jiaotong University. (Sci.) 15(3): 279-284.
19. Yamakawa, Y., K. Hashiguchi and K. Ikeda (2010). "Implicit stress-update algorithm for isotropic Cam-clay model based on the subloading surface concept at finite strains." International Journal of Plasticity 26(5): 634-658.
20. Zhang, F. (2007). "Computational Soil Mechanics [M]." Beijing: China Communications Press. (in Chinese)
21. Zhou, Y., Y. Chen, Y. Shamto and H. Hotta (2009). "Centrifuge model test on earthquake-induced differential settlement of foundation on cohesive ground." Science in China Series E: Technological Sciences 52(7): 2138-2146.